Developing a Mechanistic Understanding of Lamellar Hydroxide Mineral Carbonation Reaction Processes to Reduce CO_2 Mineral Sequestration Process Cost

Michael J. McKelvy (mckelvy@asu.edu; 480-965-4535), Andrew V. G. Chizmeshya (chizmesh@asu.edu; 480-965-6072), Hamdallah Bearat (Hamdallah.Bearat@asu.edu; 480-965-2624), Renu Sharma (Renu.Sharma@asu.edu; 480-965-4541), and Ray W. Carpenter (carpenter@asu.edu; 480-965-4549)

Center for Solid State Science and Science and Engineering of Materials PhD Program, P.O. Box 871704, Arizona State University, Tempe, Arizona 85287 USA

ABSTRACT

The potential environmental effects of increasing atmospheric CO_2 levels are of major worldwide concern. One alternative for managing CO_2 emissions is carbon sequestration: the capture and secure confinement of CO_2 before it is emitted to the atmosphere. Successful technologies must be environmentally benign, permanent, economically viable, safe and effective. As a result, their timely development represents a significant challenge.

Unlike many other proposed CO_2 sequestration technologies, which provide storage, CO_2 mineral sequestration provides permanent disposal via geologically stable mineral carbonates (e.g., $MgCO_3$). As such, mineral sequestration guarantees permanent containment and avoids adverse environmental consequences and the cost of continuous site monitoring. The major remaining challenge for CO_2 mineral sequestration is economically viable process development. This is the focus of the CO_2 Mineral Sequestration Working Group managed by DOE, which also includes members from the Albany Research Center, Los Alamos National Laboratory, National Energy Technology Laboratory, and Science Applications International Corporation.

Our goal is to develop the necessary understanding of mineral carbonation reaction mechanisms to engineer new materials and processes to enhance carbonation reaction rates and reduce process cost. Herein, we focus on Mg-rich lamellar hydroxide feedstock materials (e.g., $Mg(OH)_2$ and serpentine minerals), due to their low cost and wide availability. *In situ* dynamic high-resolution transmission electron microscopy has been used to directly observe dehydroxylation/rehydroxylation-carbonation reaction processes down to the atomic level. These studies are combined with detailed quantum mechanical modeling and a variety of complementary studies to explore the associated reaction mechanisms. Control of dehydroxylation/rehydroxylation processes prior to and/or during carbonation have been found to dramatically enhance carbonation reactivity.

INTRODUCTION

The energy infrastructure of the world is being stretched by worldwide economic expansion. The recent energy crisis in California underscores the immediate need to increase the infrastructure's capacity. As the global economy continues to expand, more and more countries will seek to attain the standard of living enjoyed by wealthier countries, further increasing worldwide energy demands.[1,2] As a result, expanding the range and capacity of energy technologies to meet these exponentially increasing energy needs is a major long, as well as short-term challenge. This challenge is further complicated by environmental concerns. Fossil fuels have long served as the major worldwide energy resource. However, this use has been predicated on the assumption that the carbon dioxide resulting from fossil fuel combustion could be freely vented to the atmosphere without adverse environmental consequences. As anthropogenic CO_2 emissions continue their exponential growth, this is no longer a clearly viable assumption. Indeed, over the past several years, discussion has shifted from whether exponentially increasing CO_2 emissions will impact the global environment, to the timing and magnitude of their impact.[1-3]

Two options are available to decrease anthropogenic CO_2 emissions: (i) expanding the role of alternative energy generation and (ii) sequestration of CO_2 emissions.[3] At present, the world's energy infrastructure is dominated by fossil-fuel-based energy generation, with 85% of global energy production based on fossil fuels. As such, alternative energy generation will not likely be able to satisfy worldwide energy needs in the foreseeable future. Fossil-fuel-based energy generation combined with CO_2 sequestration provides a potentially attractive alternative.[1-3]

Fossil fuels, in general, and coal in particular, are well positioned to supply the world's energy needs for centuries to come *if CO_2 sequestration technology can be developed that is (i) permanent, (ii) environmentally benign, and (iii) economically viable*.[1-6] There are several relatively low-cost, short-term options for CO_2 mitigation, such as improved energy generation efficiency, renewable energy sources, switching from coal to oil/gas, etc. Mid-term options include terrestrial sequestration and useful materials conversion. Although these options may be able to address short to middle term goals, buying time to develop other technologies, they are not generally viewed as long-term solutions, due to their limited mitigation capacity.[1-3]

Large-scale, long-term options being explored include ocean, geological and mineral sequestration.[1-3,7] Both ocean and geological sequestration can address the magnitude of anthropogenic CO_2 emissions via long-term storage. However, whether or not such storage can be permanent is of critical concern. Unlike ocean and geological sequestration, mineral sequestration provides permanent CO_2 disposal by forming geologically stable mineral carbonates, a process first proposed by Seifritz in 1990.[8-16] Since the materials formed already exist in vast quantities in nature, mineral sequestration can clearly provide a permanent and environmentally benign solution. Furthermore, this procedure significantly exceeds the capacity needed to sequester all the CO_2 that could be emitted from the world's known coal reserves.[5,9,13,17] Hence, mineral sequestration has the potential to provide a large-scale permanent solution, without the ongoing chronic and acute concerns associated with long-term storage, such as long-term atmospheric emission (e.g., leaking to the atmosphere, legacy concerns), sudden atmospheric release (e.g., CO_2 is a potentially lethal, heavier-than-air gas), and environmental degradation (e.g., ocean pH changes).

OBJECTIVE

The remaining goal for CO_2 mineral sequestration is economically viable process development. The permanent CO_2 disposal provided by mineral sequestration has substantial cost advantages, including avoiding the ongoing costs and liability issues associated with long-term storage. As such, the primary research objective for mineral sequestration is reducing carbonation process cost. This is the focus of the National CO_2 Mineral Sequestration Working Group managed by DOE, with members from the Albany Research Center (ARC), Arizona State University (ASU), Los Alamos National Laboratory (LANL), National Energy Technology Laboratory (NETL), and Science Applications International Corporation (SAIC).

APPROACH

Mineral carbonation of Mg-rich lamellar hydroxide based minerals (e.g., brucite, $Mg(OH)_2$ and serpentine, $Mg_3Si_2O_5(OH)_4$) is a leading CO_2 mineral sequestration process candidate currently under investigation by the Working Group.[10-12] In particular, the serpentine-based minerals are widely available in readily mineable deposits worldwide, providing the capacity to sequester all of the CO_2 that can be generated from known coal reserves.[5,9,13,17] Their low cost combined with the exothermic nature of the carbonation process (Reaction 1),[13] provide exciting potential for economically viable process development. Furthermore, mineral carbonation of serpentine-based feedstock materials can also utilize the serpentine mineral chrysotile as a feedstock material, converting hazardous waste into environmentally benign mineral products, while permanently disposing of CO_2 as magnesite, as shown in Reaction 1 for serpentine carbonation in general.

$$(1)\ Mg_3Si_2O_5(OH)_4 + 3CO_2 \rightarrow 3MgCO_3 + 2SiO_2 + 2H_2O$$

Recent ARC studies indicate aqueous solution carbonation is particularly promising.[10,18] Key to lowering process cost is the carbonation reaction rate and its degree of completion. These vary substantially depending on the feedstock, how it is pretreated, and the reaction conditions. The few available studies of this complex process show it to be quite promising, but far from optimized.[10,18] Enhancing the reaction rate and degree of completion are essential to minimizing process cost.

PROJECT DESCRIPTION

Serpentine carbonation is a very complex process, which is further complicated by the structural (e.g., lizardite, antigorite and chrysotile) and chemical complexity of these naturally occurring minerals.[19] As an initial step in understanding the dehydroxylation/carbonation mechanisms that govern these Mg-rich lamellar hydroxide based minerals, we have undertaken an investigation of the reaction mechanisms that govern dehydroxylation/carbonation behavior for the model Mg-rich lamellar hydroxide mineral brucite, $Mg(OH)_2$, due to its relative structural and chemical simplicity,[19] as described by Reaction 2.

$$(2)\ \ Mg(OH)_2 + CO_2 \rightarrow MgCO_3 + H_2O$$

$Mg(OH)_2$ is also of interest as a second step in a two-step mineral carbonation process, in which $Mg(OH)_2$ is first extracted from Mg-rich minerals.[13,14] The structural and chemical similarities between brucite and the more complex serpentine-based mineral lizardite are illustrated in Figure 1. The insight gained in these model system studies will be directly applied in our new studies of the atomic-level mechanisms that govern serpentine dehydroxylation/carbonation reaction rates, and hence, their mineral sequestration process cost.

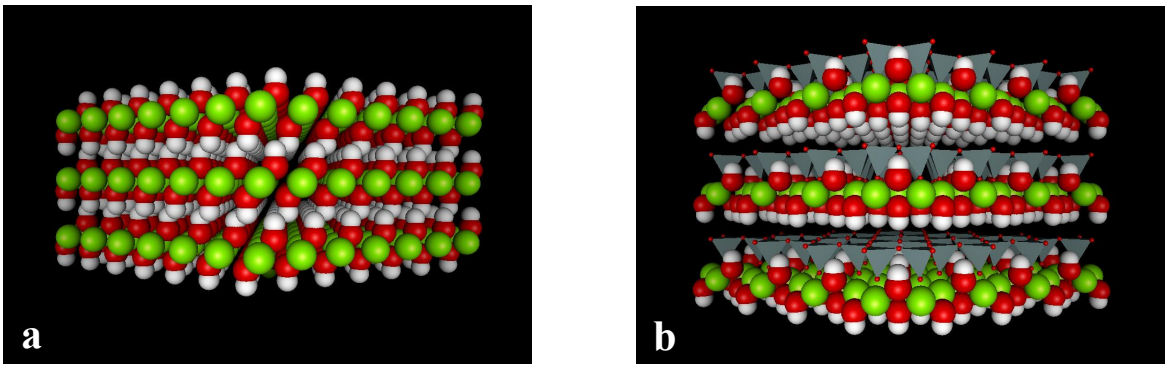

Figure 1. A lamellar view of the Mg-rich lamellar hydroxide minerals (a) brucite, $Mg(OH)_2$, and (b) serpentine (lizardite). Note the close structural similarities, with both structures containing Mg lamella and hydroxide lamella. The green, red and white spheres correspond to the Mg, O, and H atom positions, respectively. The gray tetrahedra with small red spheres at the corners correspond to the silica (SiO_4) groups connected in lamellar sheets, which also contain hydroxyl groups. Note: the structures of antigorite and chrysotile are further complicated by layer curvature, leading to much larger unit cells with modulated and coiled character, respectively.

RESULTS

$Mg(OH)_2$ Dehydroxylation: The Path to Carbonation

$Mg(OH)_2$ dehydroxylation, as described by Reaction 3, is intimately associated with the carbonation process, as water must leave the brucite crystal lattice before carbonation can occur.

$$(3) \qquad Mg(OH)_2 \rightarrow MgO + H_2O$$

Although this process has been extensively studied,[20] relatively little is known about the atomic-level mechanisms that govern dehydroxylation, especially in the early stages of dehydroxylation. The early stages are of particular interest with respect to enhancing carbonation reactivity, as CO_2 can begin to react to form carbonate locally as soon as dehydroxylation begins in that region. Recently, we have used environmental-cell (E-cell) dynamic high-resolution transmission electron microscopy (DHRTEM) to observe dehydroxylation at the atomic-level/nanoscale for the first time under a $H_2O(g)$ vapor pressure of 1 torr.[21] These studies were combined with advanced computational modeling investigations to discover that dehydroxylation proceeds via a lamellar nucleation and growth process.[21] This process can provide access to a broad solid solution series of lamellar oxyhydroxide intermediate materials during dehydroxylation. Furthermore, since dehydroxylation is a reversible process,[22] such intermediate materials may

well be accessible during rehydroxylation, as well. These intermediate materials can provide an exciting broad new range of alternative carbonation reaction pathways, as shown in Figure 2.

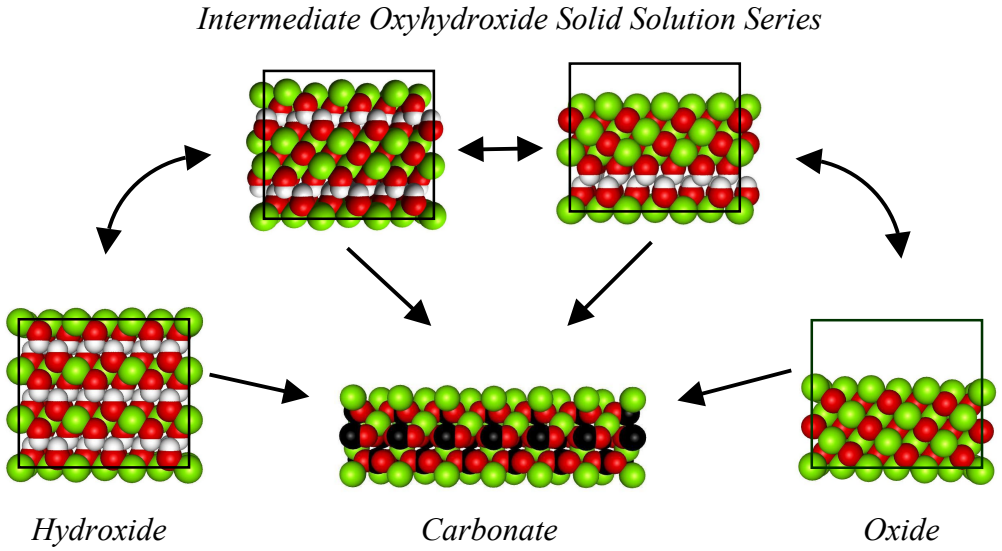

Figure 2. Possible $Mg(OH)_2$ carbonation reaction pathways during dehydroxylation and/or rehydroxylation. The lamellar structures shown are viewed parallel to their layers. Representative members of the intermediate lamellar oxyhydroxide solid solution series, $Mg_{x+y}O_x(OH)_{2y}$, are shown. The constant size black outlines are provided as a guide to the eye to emphasize the dramatic reduction in interlayer spacing, and volume, that occurs during dehydroxylation. The Mg, O, H, and C atom positions are depicted by the green, red, white, and black spheres, respectively. $MgO/Mg(OH)_2$ can form via low-temperature dehydroxylation/rehydroxylation, respectively (potentially cycling back and forth at low temperatures). Carbonate formation from any of these materials is thermodynamically dictated as a one way reaction below the $MgCO_3$ decomposition temperature.[23]

Advanced computational modeling shows the free energy of formation of these intermediate materials is within 1-2 kcal/mol of the stoichiometric equivalent amount of $MgO + Mg(OH)_2$, underscoring the kinetic/thermodynamic accessibility of these materials via lamellar nucleation and growth under typical reaction conditions.[21]

In addition to being able to access new lamellar oxyhydroxide intermediate materials, dehydroxylation can also dramatically affect the morphology of the feedstock material. During dehydroxylation, the $Mg(OH)_2$ matrix collapses by ~50% perpendicular to its host lamella and contracts by ~ 5% parallel to the lamella. The elastic strain associated with this contraction can induce a variety of morphological changes, including internal blister formation between the host $Mg(OH)_2$ layers, lamellar and translamellar cracking down to the nanoscale (nano-fracture) and morphological reconstruction of the resulting fragmented matrix to form high-surface-area materials, with surface areas in excess of 100 m^2/g.[11,21,24] Our integrated DHRTEM, optical microscopy and field-emission scanning electron microscopy observations suggest all of these phenomena, as well as intermediate oxyhydroxide formation, are related to the lamellar nucleation and growth process that governs $Mg(OH)_2$ dehydroxylation. As seen in Figure 3, competition between slow nucleation and rapid growth and rapid nucleation and slow growth

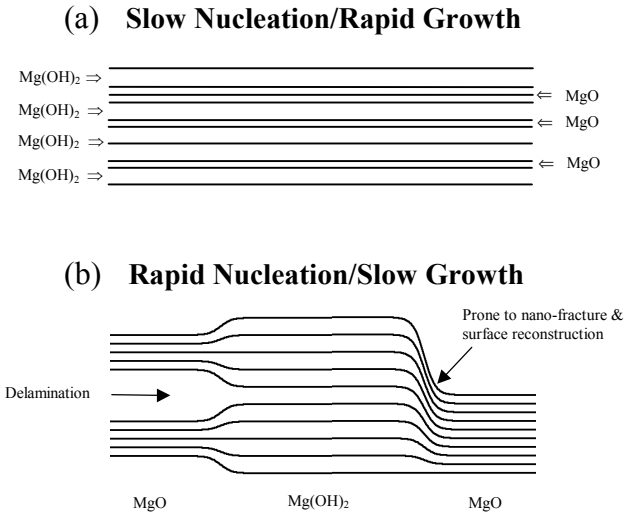

Figure 3. Models of lamellar nucleation and growth processes during $Mg(OH)_2$ dehydroxylation.[21] A model for relatively slow nucleation and rapid growth leading to oxyhydroxide intermediate formation is shown in (a). The process proceeds in a largely homogeneous fashion locally. A model for relatively rapid nucleation and slow growth leading to primarily two-phase, $Mg(OH)_2$ + MgO, dehydroxylation behavior is shown in (b).

processes can promote lamellar oxyhydroxide intermediate formation and local two-phase, MgO + $Mg(OH)_2$, formation, as well as nano-fracture of the host matrix.[21] Higher and lower reaction temperatures are generally expected to favor nucleation and growth, respectively. This suggests the exciting possibility of controlling carbonation reaction intermediate formation via controlled dehydroxylation. Nano-fracture also provides the high-surface areas needed to induce morphological reconstruction to form the well-known nanostructured materials that can result from extensive $Mg(OH)_2$ dehydroxylation.[21] We have also observed internal blister formation early in the dehydroxylation process via optical microscopy, as shown in Figure 4, with the blisters soon becoming a part of the nano-fractured host matrix as crystal fracture propagates throughout the dehydroxylating matrix.[24]

Figure 4. Typical internal blister formation observed perpendicular to the single-crystal $Mg(OH)_2$ basal plane surface early during dehydroxylation/dehydroxylation-carbonation reaction processes. As dehydroxylation continues, host-matrix cracking disrupts the blisters as the matrix is fractured down to the nanoscale.

Cumulatively, the $Mg(OH)_2$ host matrix can be viewed as becoming a highly porous pseudomorphic structure during dehydroxylation, with the ability to locally form a broad range of lamellar oxyhydroxide intermediate materials during the dehydroxylation process.

$Mg(OH)_2$ Dehydroxylation/Rehydroxylation-Carbonation Reaction Mechanisms:

The timing and relationship between dehydroxylation and carbonation reaction mechanisms during direct carbonation can dramatically affect carbonation reaction rates. For example, dehydroxylation may occur too rapidly relative to carbonate formation. Such conditions could favor MgO sintering/particle-size growth (which may be aided by the water vapor formed),[14] inhibiting carbonation reactivity in the process. Similarly, very slow dehydroxylation may also inhibit carbonation via passivating carbonate layer formation.[14] On the other hand, the nano-fracture and morphological reconstruction associated with dehydroxylation together with oxyhydroxide intermediate formation may enhance carbonation reaction rates by (i) creating intermediate materials with enhanced carbonation reactivity, (ii) dramatically increasing the sample surface area, (iii) creating fresh carbonation reaction sites as dehydroxylation progresses, and (iv) fracturing and disrupting any passivating carbonate layers that may form.[21,24]

In order to determine the overall impact of the above dehydroxylation/carbonation reaction mechanisms on carbonation reactivity, we have carried out a series of dehydroxylation-carbonation experiments as a function of CO_2 reaction pressure at 585 ^oC.[24] The extent of carbonation and dehydroxylation (total MgO + $MgCO_3$), as determined by C and H elemental analysis, are shown in Figure 5. As for all of our dehydroxylation-carbonation studies, the extent of dehydroxylation significantly exceeds the extent of carbonation, indicating dehydroxylation and carbonation are separate, but intimately related processes. Although $MgCO_3$ is unstable below the critical carbonation pressure (~789 psi at 585 ^oC)[14,23,24] with respect to MgO and CO_2, the greatest extent of carbonate formation was observed in the subcritical pressure region. This suggests these samples exhibit dramatically enhanced carbonation reactivity on cooling, which occurs over approximately 30 minutes.

To confirm carbonation occurs on cooling in the subcritical pressure region, samples were temperature quenched and evacuated immediately after reaction at 585 ^oC from above and below the critical carbonation pressure, as shown by the squares in Figure 5. The sample quenched in the subcritical pressure region exhibited substantially less carbonation (just within experimental error of zero), whereas the sample quenched from above the critical carbonation pressure exhibited the extent of carbonation expected for carbonation occurring at 585 ^oC. Consequently, dramatically higher carbonation reaction rates are present on cooling in the subcritical pressure region, even though the activation energy available for carbonation decreases dramatically with sample cooling. The dramatic increase in carbonation reactivity is likely associated with lattice fracture and morphological reconstruction during extensive dehydroxylation at 585 ^oC, forming carbonation-reactive, high-surface-area intermediate materials, prior to cooling.[21,24] The increase in carbonation extent with increasing CO_2 pressure in the subcritical pressure region can be associated with (i) the increase in CO_2 activity with increasing pressure and (ii) the broader temperature range over which carbonation can occur on cooling.

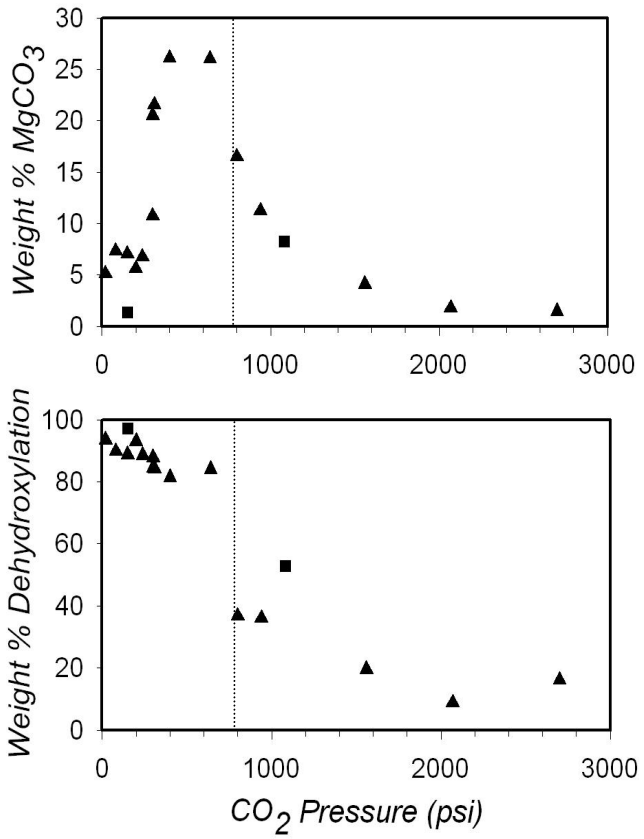

Figure 5. Wt % $MgCO_3$ formed (above) and wt% dehydroxylation (wt.% MgO + wt.% $MgCO_3$; below) vs. CO_2 pressure for similarly-sized $Mg(OH)_2$ single crystal fragments reacted at 585ºC (±5ºC) for 16 hours. Triangles represent reactions in which the autoclave was air-cooled (~ 30 min), while the sample was still under CO_2, to ambient temperature at the end of each run. Squares represent reactions in which the autoclave was water quenched, immediately followed by CO_2 evacuation at the end of each run. The critical carbon dioxide pressure for $MgCO_3$ formation at 585 ^oC is shown by the dotted line (~ 789 psi).[24,25]

That extensive dehydroxylation does occur at 585 ^oC, is confirmed by the extensive dehyroxylation exhibited by both the quenched and unquenched samples in the subcritical pressure region. Similar dehydroxylation processes are well known to result in extensively-dehydroxylated, high-surface-area materials, which can also exhibit ambient temperature rehydroxylation behavior.[22]

We have combined thermogravimetric analysis (TGA, ambient pressure), elemental analysis of the intermediate and final materials formed, and surface area (BET) studies of similar dehydroxylation/rehydroxylation-carbonation processes to explore the carbonation reactivity of extensively dehydroxylated $Mg(OH)_2$ intermediate materials.[24] $Mg(OH)_2$ single-crystal fragments were initially dehydroxylated to a similar extent as the samples in the subcritical pressure region of Figure 5 (~90% dehydroxylation) under helium at 375 ^oC. This resulted in samples with surface areas of ~120 m^2/g. Subsequent exposure to humid (~80% humidity) and dry CO_2 at 375 ^oC resulted in ~2 wt % carbonate formation, after which carbonation ceased. This indicates that although the extensively dehydroxylated intermediate material has a very high surface area, only a limited number of carbonation reactive sites are accessible at 375 ^oC. However, on cooling to ambient temperature under humid CO_2, the carbonation reactivity increases dramatically,

together with some rehydroxylation. Rehydroxylation appears to stimulate carbonation by creating new carbonation-reactive intermediate materials (e.g., lamellar oxyhydroxides) and sites, which take advantage of the high-surface-area intermediate materials formed via extensive dehydroxylation. These observations, together with those in Figure 5 (where $H_2O(g)$ from dehydroxylation remains in the autoclave on cooling), demonstrate that the high surface area of extensively dehydroxylated $Mg(OH)_2$ can combine with rehydroxylation intermediate formation to dramatically enhance carbonation reactivity, *even at ambient temperature*.

Increasing the carbonation reaction pressure beyond the critical CO_2 pressure needed for $MgCO_3$ formation results in a sudden decrease in the extent of carbonation and dehydroxylation. This is likely associated with the formation of passivating carbonate layers during dehydroxylation-carbonation at 585 ^oC, as observed in our recent secondary ion mass spectrometry study.[24] As suggested previously, such passivating carbonate layer formation can significantly impede both dehydroxylation and carbonation.[14] However, as discussed above, concurrent dehydroxylation mechanisms, such as cracking of the host matrix and morphological reconstruction down to the nanoscale, can disrupt any carbonate layers that form, providing new H_2O and CO_2 diffusion pathways that can physically bypass the carbonate layers and facilitate carbonation.

Above the critical CO_2 pressure needed for carbonate formation, entirely different reaction mechanisms govern the carbonation process. This is evidenced by the dramatic *decrease in carbonation reactivity with increasing CO_2 activity/pressure* in Figure 5. In this pressure region, dehydroxylation occurs together with, rather than prior to, carbonation, with the rate of dehydroxylation also decreasing with increasing pressure. The slowing of dehydroxylation and carbonation with increasing pressure can be directly associated with the decrease in the diffusion rate of (i) $H_2O(g)$ out of and (ii) $CO_2(g)$ into the porous reaction matrix with increasing CO_2 pressure. Dehydroxylation is slowed due to the higher local pressure of H_2O present near the dehydroxylating reaction sites. Carbonation, in turn, is slowed by the slower rate of dehydroxylation and is further inhibited by the slower rate of CO_2 diffusion to the carbonation reactive intermediate sites that form. The decrease in dehydroxylation with increasing CO_2 pressure in the subcritical pressure region of Figure 5 similarly follows, since dehydroxylation occurs at reaction temperature (585 ^oC) prior to cooling, where increasing CO_2 pressures again serve to decrease the diffusion rate of H_2O away from the reaction matrix.

We have further explored the intriguing ability of extensively dehydroxylated $Mg(OH)_2$ to exhibit enhanced ambient temperature carbonation reactivity via E-cell DHRTEM studies of the *in situ* rehydroxylation-carbonation process. The E-cell HRTEM system is the same system used in our previous studies of the *in situ* $Mg(OH)_2$ dehydroxylation process.[21] Single crystal fragments were loaded into the microscope and initially imaged under a $H_2O(g)$ atmosphere, as shown in Figure 6a. The samples were then heated to 480 ^oC in the microscope vacuum in the absence of the electron beam to generate extensively dehydroxylated $Mg(OH)_2$. The sample was then cooled to ambient temperature and exposed to 400 millitorr of humid CO_2, while imaging the reaction, as shown in Figures 6b-d. An amorphous material (an evidenced by selected area electron diffraction) immediately begins to grow from the extensively dehydroxylated $Mg(OH)_2$. The amorphous material forms and grows quite rapidly, as seen in Figures 6b-d. Parallel electron energy loss spectroscopy (PEELS) was used to further characterize the amorphous material formed, as shown in Figure 7. The strong similarities between the C K-edge spectra

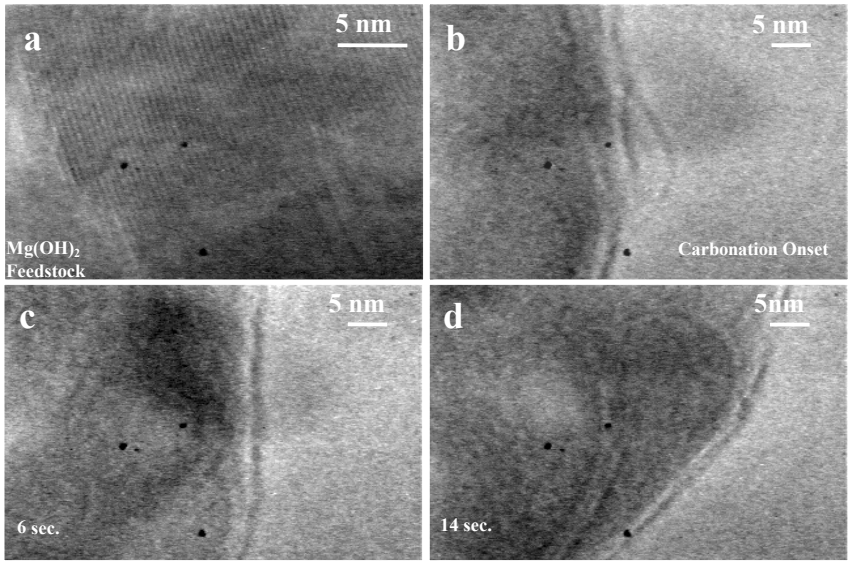

Figure 6. *In situ* E-cell DHRTEM observation of the ambient temperature carbonation-rehydroxylation process for extensively dehydroxylated $Mg(OH)_2$; a) image of the initial $Mg(OH)_2$ layers under ~1 torr $H_2O(g)$ prior to extensive dehydroxylation at 480 ^oC in the microscope vacuum; b) initial reaction of the extensively dehydroxylated $Mg(OH)_2$ upon exposure to 400 millitorr of humid CO_2 at ambient temperature; c and d) reaction progress as a function of time.

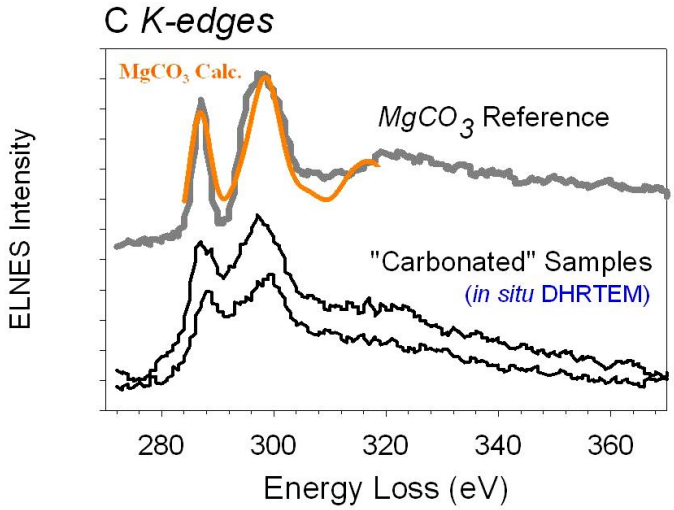

Figure 7. C K-edge energy loss near-edge structure (ELNES) observed during *in situ* ambient temperature carbonation-rehydroxylation of extensively dehydroxylated $Mg(OH)_2$. Note the good agreement between the experimental and theoretical $MgCO_3$ (magnesite) ELNES spectra and the spectra observed for the ambient temperature carbonation product.

observed for the amorphous material formed and those observed experimentally and calculated theoretically for magnesite ($MgCO_3$) indicate that the ambient temperature reaction product is indeed an amorphous carbonate. This carbonate may well contain hydroxyl groups as well, as our combined TGA and elemental analysis studies, discussed previously, indicate that some rehydroxylation occurs together with carbonation.

Summary

$Mg(OH)_2$ carbonation was chosen as a model Mg-rich lamellar hydroxide mineral carbonation system to begin to develop an atomic-level understanding of the mechanisms that govern dehydroxylation/rehydroxylation-carbonation processes for this important class of minerals. $Mg(OH)_2$ dehydroxylation and carbonation are separate but closely interrelated reaction processes. $Mg(OH)_2$ dehydroxylation is best described as a lamellar nucleation and growth process that can lead to a solid solution series of lamellar oxyhydroxide intermediate materials with potentially enhanced carbonation reactivity, as shown in Figure 2. Similar intermediate materials may also form during rehydroxylation, providing similar new reaction pathways for rehydroxylation-carbonation processes. Dehydroxylation mechanisms can also induce a variety of morphological changes, including crystal fracture and morphological reconstruction down to the nanoscale, that can (i) dramatically increase the sample surface area, (ii) create fresh carbonation reaction sites as dehydroxylation progresses, and (iii) fracture and disrupt any passivating carbonate layers that may form. The above mechanisms directly govern the observed carbonation reactivity of $Mg(OH)_2$. The reaction rates for direct $Mg(OH)_2$ carbonation are optimized at CO_2 reaction pressures that just exceed the minimum pressure needed to stabilize $MgCO_3$ formation. Progressively higher reaction pressures increasingly inhibit dehydroxylation and carbonation by slowing H_2O diffusion away from and CO_2 diffusion to the reaction sites in the porous reaction matrix that forms, respectively. Controlled application of the above mechanisms can also result in dramatically enhanced carbonation reactivity via controlled rehydroxylation-carbonation for low-temperature dehydroxylated $Mg(OH)_2$, *even at ambient temperature.*

APPLICATION

The major advantages of CO_2 mineral sequestration are its ability to guarantee permanent and environmentally benign CO_2 disposal. It also has more than the capacity needed to dispose of all of the CO_2 that could be generated from the world's known coal reserves, providing the ability to serve as a large-capacity, long-term sequestration option. Other large-capacity, long-term options, such as ocean and geological sequestration, focus on long term CO_2 storage. Unfortunately, these options have ongoing chronic and acute concerns associated with both the permanence of the proposed storage and its associated environmental impact. Issues such as long-term atmospheric emission (e.g., leaking to the atmosphere, legacy concerns), sudden atmospheric release (e.g., CO_2 is a potentially lethal, heavier-than-air gas), and environmental degradation (e.g., ocean pH changes) are of substantial concern. Mineral sequestration not only avoids these concerns, it also avoids the ongoing costs associated with long-term environmental monitoring and mitigating any environmental damage that may occur. It also avoids any costs associated with sudden catastrophic releases, which, for example, can endanger human life.[13,26]

Consequently, the major goal for CO_2 mineral sequestration is economically viable process development. The process currently showing the best potential for economic viability is the aqueous mineral carbonation process developed by the Albany Research Center, which uses serpentine and/or olivine-based minerals as the feedstock material. Although this process has already achieved good conversion rates (e.g., less than a hour), the process is definitely not optimized. At present, the best conversion rates have been observed for heat pretreated serpentine. However, this is an energy intensive process step. Efforts are currently underway to bypass the heat pretreatment step (without reducing mineral to carbonate conversion rates), which can cut the overall process energy use in half. Economic viability will also be enhanced via development of a continuous process that can operate at relatively low reaction pressures.

FUTURE ACTIVITIES

Enhancing carbonation reaction rates are key to economically viable process development. Key to being able to engineer improved feedstock materials and processes to enhance carbonation reactivity, is developing an atomic-level understanding of the mechanisms that govern carbonation and its associated reaction processes. In our future activities at Arizona State University, we will focus on extending our atomic-level understanding of the mechanisms that govern dehydroxylation/rehydroxylation-carbonation processes for the model Mg-rich lamellar hydroxide mineral $Mg(OH)_2$ to the substantially more complex serpentine-based minerals (antigorite, lizardite and chrysotile). We will explore both the heat pretreatment process and how it enhances the carbonation reactivity of serpentine. This understanding will then be used to help engineer lower cost pretreatment processes to enhance serpentine carbonation reactivity. We will also explore the mechanisms that govern the aqueous solution carbonation reactivity of serpentine-based feedstock materials via *in situ* and *ex situ* techniques to better understand the mechanisms that govern their carbonation reaction rates.

REFERENCES

1. Herzog, H.; Drake, E.; Adams, E. *CO_2 Capture, Reuse, and Storage Technologies for Mitigating Global Climate Change*, DOE Report No. DE-AF22-96PC01257 (1997).
2. *Carbon Sequestration Research and Development*, Offices of Science and Fossil Energy, U.S. Department of Energy (December 1999).
3. Halmann, M.; Steinberg, M. *Greenhouse Gas Carbon Dioxide Mitigation, Science and Technology*, Lewis Publishers, London, 1999.
4. Current estimates of world coal reserves are 10,000 billion tons. Less than 0.1% is currently consumed annually (see references 5 and 6).
5. United Nations, *1991 Energy Statistics Yearbook*, New York, 1993.
6. Climate Change 1995: *The Science of Climate Change*. Contribution of Working Group I to the Second Assessment Report of the Intergovernmental Panel on Climate Change, Cambridge University Press, 1995.
7. Lackner, K.; Grimes, P. ; Ziock, H. Los Alamos National Laboratory Technical Report LA-UR-99-583.
8. Seifritz, W. *Nature* **345**, 486 (1990).
9. Lackner, K.; Wendt, C.; Butt, D.; Joyce Jr., E.; Sharp, D.; *Energy* **20**, 1153-70 (1995).

10. O'Connor, W. K.; Dahlin, D. C.; Nilsen, D. N.; Walters, R. P.; Turner, P. C. *Proceedings of the 25th International Technical Conference on Coal Utilization & Fuel Systems* (Clearwater, Florida, March 2000), pp. 153-64. Edited by Barbara A. Sakkestad, Coal Technology Association, Rockville, MD, 2000.
11. McKelvy, M. J.; Sharma, R.; Chizmeshya, A. V. G.; Bearat, H.; Carpenter, R.W. *Proceedings of the 25th International Technical Conference on Coal Utilization & Fuel Systems* (Clearwater, Florida, March 2000), pp. 897-908. Edited by Barbara A. Sakkestad, Coal Technology Association, Rockville, MD, 2000.
12. McKelvy, M. J.; Chizmeshya, A. V. G.; Bearat, H.; Sharma, R.; Carpenter, R.W. *Proceedings of the 17th International Pittsburgh Coal Conference* (Pittsburgh, PA, September 2000), section 18A, pp. 8-20. Pittsburgh Coal Conference, University of Pittsburgh, Pittsburgh, PA, 2000.
13. Lackner, K.; Butt, D.; Wendt, C.; Goff, F.; Guthrie, G. Los Alamos National Laboratory Technical Report LA-UR-97-2094 (1997).
14. Butt, D. P.; Lackner, K. S.; Wendt, C. H.; Conzone, S. D.; Kung, H.; Lu, Y.-C.; Bremser, J. K. *J. Am. Ceram. Soc*., **79** [7] 1892-98 (1996).
15. Butt, D. P.; Lackner, K. S.; Wendt, C. H.; Benjamin, A. S.; Currier, R.; Harradine, D. M.; Holesinger, T. G.; Park, Y. S.; Rising, M. *World Resource Review*, **9** [3], 324-36 (1997).
16. McKelvy, M. J.; Chizmeshya, A. V. G.; Bearat, H.; Sharma, R.; Carpenter, R.W. *Proceedings of the 26th International Technical Conference on Coal Utilization & Fuel Systems* (Clearwater, Florida, March 2001), submitted.
17. Lackner, K.; Butt, D.; Wendt, C.; Sharp, D. *Proceedings of the 21st International Technical Conference on Coal Utilization & Fuel Systems*, pp. 133-44. Edited by Barbara A. Sakkestad, 1996.
18. O'Connor, W.; Dahlin, D.; Rush, G.; Dahlin, C.; and Collins, W. *Proceedings SME 2001* (in press).
19. See, for example, Klein, C.; Hurlbert, C.S. *Manual of Mineralogy*, 21st edn (Wiley, New York, 1993).
20. See, for example, references in references 14 and 21.
21. McKelvy, Michael J.; Sharma, R.; Chizmeshya, Andrew V.G.; Carpenter, Ray W.; Streib, Ken *Chem. Mater*. (in press).
22. Ribeiro Carrott, M.M.L.; Carrott, P.J.M. *Characterization of Porous Solids III*, Studies in Surface Science and Catalysis, **87**, 497-506 (1994).
23. Harker; R. I.; Tuttle, O. F. *Am. J. Sci.* **253**, 209-24 (1955).
24. Bearat, H.; McKelvy, M. J.; Chizmeshya, A. V. G.; Sharma, R.; Carpenter, R.W. (submitted).
25. The critical CO_2 pressure for $MgCO_3$ formation/decomposition as a function of temperature is estimated from a $\ln P(CO_2)$ vs. $1/T(K)$ plot of the $MgCO_3 \Leftrightarrow MgO + CO_2$ decomposition/formation P vs. T data available in references 14 and 23.
26. Kling, G.; Clark, M.; Compton, H.; Devine, J.; Evans, W.; Humphrey, A.; Koenigsberg, E.; Lockwood, J.; Tuttle, M.; Wagner, G. *Science* **236**, 169-75, (1987).